

Optimising Low Molecular Weight Hydrogels for Automated 3D Printing†

Michael C. Nolan,^{a,b} Ana M. FuentesCaparrós,^{a,c} Bart Dietrich,^a Michael Barrow,^b Emily R. Cross,^a Markus Bleuel,^{d,e} Stephen M. King,^f and Dave J. Adams^a

^a *School of Chemistry, University of Glasgow, Glasgow, G12 8QQ, UK. E-mail: dave.adams@glasgow.ac.uk*

^b *Department of Chemistry, University of Liverpool, Liverpool L69 7ZD, UK*

^c *Department of Chemical Engineering, Faculty of Sciences, 18071 Granada, Spain*

^d *NIST Center for Neutron Research, National Institute of Science and Technology, Gaithersburg, MD 20988-8562, US*

^e *Department of Materials Science and Engineering, University of Maryland, College park, MD 20742-2115, US*

^f *STFC Pulsed Neutron and Muon Source, Science and Technology Facilities Council, Rutherford Appleton Laboratory, Harwell Campus, Didcot, OX11 0QX, UK*

Supporting Information

Experimental

3D Printer: The 3D printing of gels was carried out on a RepRap Ormerod 2 3D printer version 528.4 (<https://reprappro.com/documentation/ormerod-2/>) running David Crocker's dc42 firmware version 1.09k (<https://github.com/dc42/RepRapFirmware>). The hot end and extruder drive of the printer were replaced with a paste extruder designed by Richard Horne (<http://richrap.blogspot.co.uk/2012/04/universal-paste-extruder-ceramic-food.html>). The printer was controlled *via* a modified version of Christian Hammacher's Duet Web Control user interface version 1.06 (<https://github.com/chrishamm/DuetWebControl>). A number of modifications to the printer's startup configuration file were necessary to accommodate the paste extruder.

Principles: The RepRap Ormerod 2 3D printer executes instructions from a subset of G-code, a common scripting language for industrial CNC applications. The user interface translates user commands (e.g. move print head forward along x-axis by 1 mm) into G-code (G91 G1X1) and sends it to the printer's microcontroller. The microcontroller firmware in turn translates this into a pulse sequence to be sent to the x-axis stepper motor to move the print head. The number of pulses in this sequence is directly related to the number of rotational steps that the stepper motor shaft will advance, and hence the extent of movement along the axis. The filament extruder is treated as a fourth, though infinite axis. Movement along this axis constitutes the extrusion (or retraction) of filament, and the magnitude of the movement refers to the length of filament extruded (or retracted). For the present application, we needed to adapt the printer to work with the paste extruder rather than the usual filament extruder. The behaviour of the x, y, and z movement axes would not be affected and did not require any modifications.

The specifications of the stepper motor in the paste extruder are largely identical to those in the filament extruder, the motor uses the same electrical connection to the microcontroller board, and has an identical response to a pulse train from the microcontroller. So far as the electronic hardware is concerned, they are interchangeable and the microcontroller does not care which one it is driving. This removes the need for any electrical or firmware modifications.

The relationship between rotation of motor shaft and length of filament extruded is a function of motor steps/revolution and any gear ratios in the extruder. This relationship is linear, and can therefore be treated as a "black box" and expressed conveniently as a single scaling factor. This scaling factor is used in normal printer operation to calibrate axis (or extruder) motions when a different motor or set of gears is fitted. Calibrating fluid volumes dispensed by the paste extruder is therefore merely a matter of scaling the pulse count to some chosen volumetric base unit. Conveniently, the firmware allows for this in a single command.

The base unit for axis movement and filament extrusion is the millimetre. For paste extruder operation, we chose to equate one millimetre of filament to 1 μL of fluid. In other words, commanding the printer to extrude 1 mm of filament should expel 1 μL of fluid from the paste extruder. This choice was entirely arbitrary and any other volumetric unit (or multiple thereof) could have been chosen.

The paste extruder and hardware modifications: The significantly larger inertial mass of the gel extruder compared to the usual hot end combined with the anticipated higher required acceleration and deceleration rates and hence the stress that the x-axis would be subjected to, necessitated the replacement of the original acrylic x-axis arm of the printer with a sturdier aluminium version. This was obtained from DD Metal Products at <https://ddmetalproducts.co.uk/product/x-axis-arm-kit/>.

The paste extruder was printed in PLA (polylactic acid filament) and assembled as described in the source (Fig. S1). To fit the paste extruder to the RepRap Ormerod 2's x-axis, a caddy system was designed and printed (Fig. S2). The design files for the caddy can be supplied on request. The hot end, infrared sensor board and nozzle mount were removed from the x-axis carriage (Fig. S3) and the filament extruder drive was disconnected and removed from the x-axis arm. The caddy was fitted to the bare x-axis carriage via two M3 bolts and washers (Fig. S4). Finally, the paste extruder was attached to the caddy via two M4 bolts self-tapping into the holes in its base and connected to the microcontroller board in place of the filament extruder drive (Fig. S5). A runner bearing mounted on the caddy takes some of the weight of the paste extruder assembly off the x-axis carriage and transfers it to the aluminium x-axis rib (Fig. S6). An 11 mm diameter bearing was used herein but any reasonably sized bearing will work since the height of the runner mount is adjustable. The syringe and gel loaded into the printer ready to print is shown in Fig. S7.

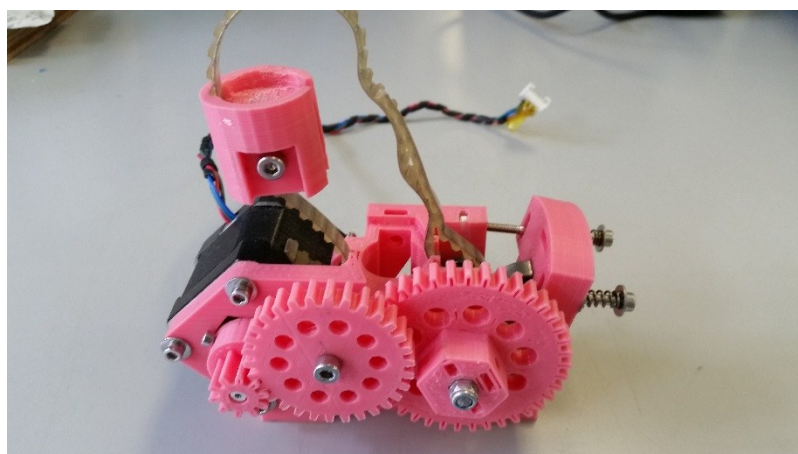


Figure S1. The paste extruder.

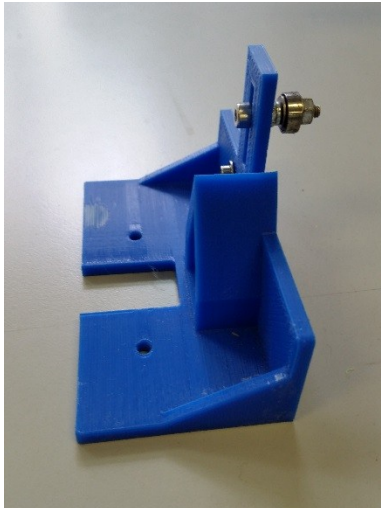


Figure S2. Paste extruder caddy.

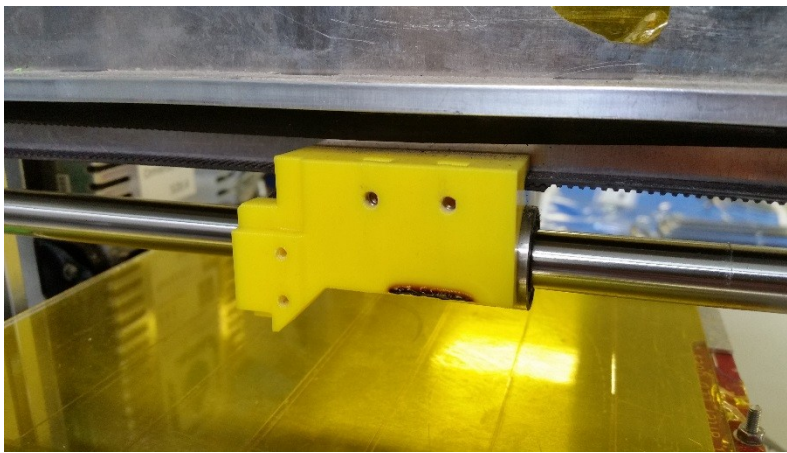


Figure S3. Bare x-axis carriage with hot end, infrared sensor board, and nozzle mount removed.

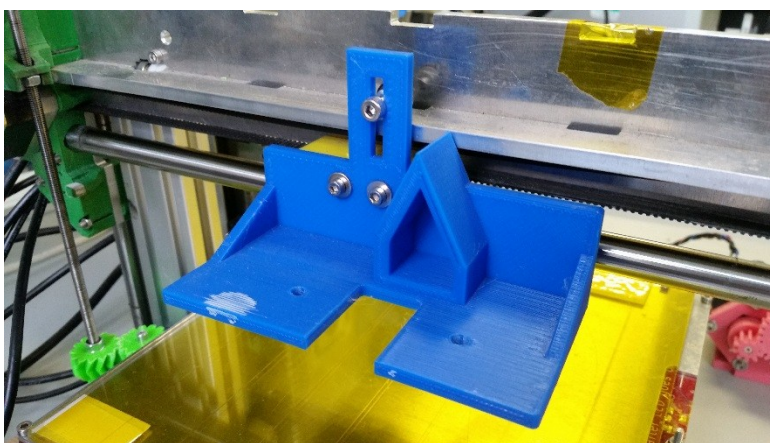


Figure S4. Caddy mounted to the x-axis carriage.

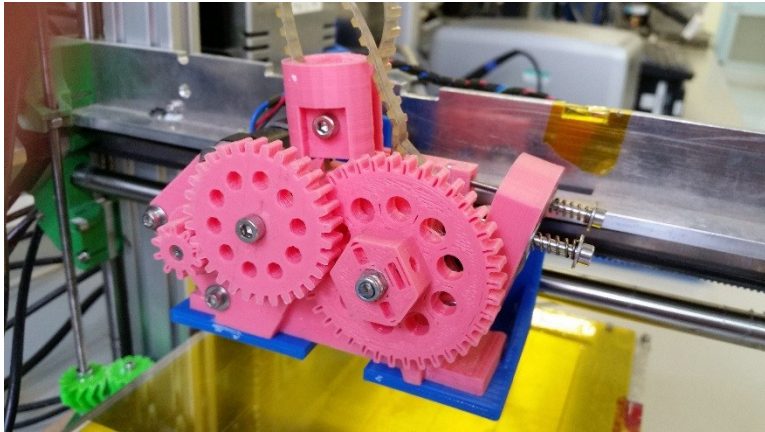


Figure S5. Paste extruder mounted on caddy.

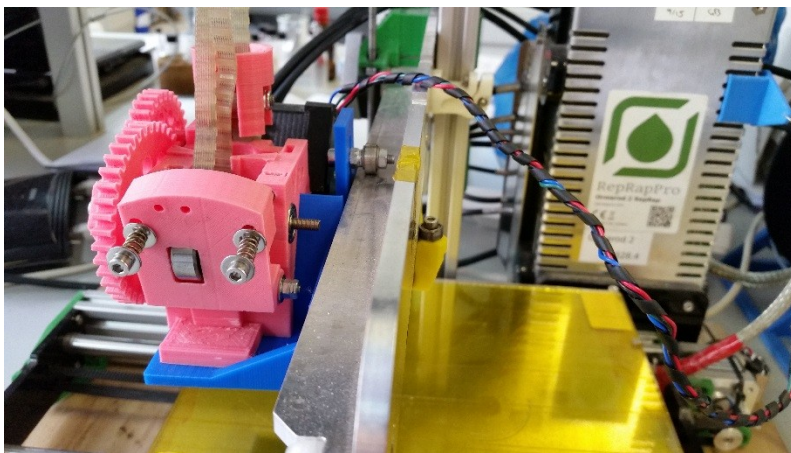


Figure S6. Caddy runner bearing riding atop x-axis rib (left of vertical x-axis arm) and x-axis carriage runner bearing (right of x-axis arm).

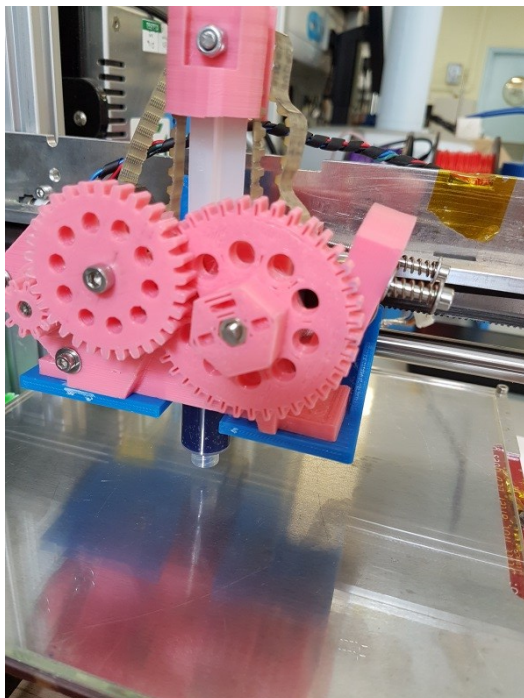


Figure S7. The syringe and gel loaded into the paste extruder ready to be extruded onto the printing bed.

Modifications to the printer's startup configuration file: When the printer is powered up, it reads and executes the "config.g" file in its SD card's "\sys" folder. This file holds start-up settings and default parameters. A number of these required modification to accommodate the paste extruder. The appropriate G-code is given in parentheses in the following. More information can be found in the RepRap G-code reference (<http://reprap.org/wiki/G-code>). A copy of our config.g file can be supplied on request.

The large mass of the paste extruder combined with high accelerations could result in the stepper motor skipping steps along the x-axis. Similarly, surface irregularities in the 3D printed paste extruder could result in variable torque requirements as its gears revolve, leading to skipped steps in the extruder motor. For these reasons, the x-axis and extruder motor currents were increased to 1200 mA (M906).

The extruder axis direction was inverted (M569)

The axis_steps_per_unit parameter was set to the appropriate number of stepper motor steps required for the extrusion of 1 μL of fluid (M92). The calibration procedure is described below.

In normal operation, all axis and extruder motor movements initiate and terminate with controlled acceleration and deceleration, resulting in smooth motion of the print head and little frame vibration. Each axis (and extruder) has its own maximum acceleration setting, and the lowest of these determines the overall acceleration/deceleration for a given movement combination. The amount of plastic extruded along the way (if any) is scaled accordingly. In the context of printing gels however, the extrusion rate determines shear, which in turn determines the final properties of the extruded gel. From this standpoint, acceleration and deceleration are undesirable as gel extruded during acceleration/deceleration could conceivably possess different properties to gel extruded during full-speed movement. While the acceleration/deceleration periods cannot be eliminated, they can be kept short, at the expense of axis vibration, jerky movements, and the steppers possibly skipping steps. The x-, y-axis and extruder motor accelerations were therefore increased to 4000 mm/s^2 , 2000 mm/s^2 and 30000 $\mu\text{L/s}^2$, respectively (M201).

The maximum x and y-axis and extruder motor speeds were increased to 30000 mm/min , 30000 mm/min , and 60000 $\mu\text{L/min}$, respectively (M203).

The minimum extruder motor speed parameter was increased to 600 $\mu\text{L/min}$ (M566).

The extruder heater was removed from the extruder tool definition (M563).

The extruder drive was set to active by default (T0).

Cold-extrusion prevention was disabled (M302).

The volume calibration (M92) of the paste extruder was carried out as follows. Using the original M92 parameter value (motor steps per millimetre of filament), a syringe of water fitted with a needle was loaded into the paste extruder and the printer was instructed to extrude increasing “lengths of filament” into vials, until the actual volume of water extruded was close to 1 g (therefore 1 mL). The approximate new value of the M92 (axis_steps_per_unit) parameter required to make 1 microlitre the base unit was calculated by linear extrapolation from the current axis_steps_per_unit value, the actual amount of water dispensed, and the “length of filament” which resulted in a volume close to 1 mL. The M92 setting was then updated via the user interface. With the printer’s base unit now being approximately 1 μL , the printer was instructed to dispense 1000 μL (G-code command G1E1000) of water into 10 pre-weighed vials. The amounts dispensed were weighed and averaged. A refined axis_steps_per_unit value was calculated as above and updated in the “config.g” file. For reference, the value of the M92 parameter for normal printer operation is around 400, while for gel extrusion it was less than 10. The accuracy of the paste extruder was subsequently verified to be better than $\pm 5\%$ and repeatable for volumes of the order of 1 mL.

Modifications to the user web interface: The file “regrap.htm” in the folder “\www” on the printer’s SD card is loaded by the controlling computer’s browser when connecting to the printer, and constitutes the front end of the user interface (“Duet web control”, released under the terms of the GNU General Public License 2.0, <http://www.gnu.org/licenses/gpl-2.0.html>). This allows moving of the print head, setting movement speeds, controlling the heaters, extruding and retracting filament, and uploading files to the printer to be printed.

The extruder section of the control interface was of interest to us. This section contains buttons for the extrusion (or retraction) of set lengths (millimetres) of filament and setting of the feed rate (in mm/s). Even though the gel patterns printed in the present work were programmed as short G-code scripts and uploaded directly to the printer, the control buttons were useful for loading (and unloading) and priming syringes containing gels, and calibrating the paste extruder.

The changes made to the “regrap.htm” file were as follows. The button section headers were changed from “Feed amount in mm” to “Feed amount in mL”, and from “Feedrate in mm/sec” to “Feedrate in $\mu\text{L}/\text{sec}$ ”, respectively. The original control buttons for feed amount are labelled 1, 5, 10, 20, 50, and 100 mm, and 5, 10, 20, 40, and 60 mm/s for feed rate. For paste extruder usage, the button labels for feed amount were changed to 0.01, 0.05, 0.1, 0.2, 0.5, and 1 mL. Similarly, the button labels for feed rate were changed to 50, 100, 200, 500, and 1000 $\mu\text{L}/\text{sec}$. The button

values were changed as required for the new base unit (the microlitre): for a feed amount of 0.05 mL, the button value in the HTML code should read 50, while the new button values for the feed rate were identical to the new button labels, as both are in microlitres. The code section where these amendments were made begins at line 573 in the original “regrap.htm”. Optional cosmetic changes to the title bar and the page name reported to the browser were made near the top of the HTML file. A copy of our modified regrap.htm file can be supplied on request.

The file “interface.js” in folder “\www\js” on the printer’s SD card contains the JavaScript code for event handlers and functions called from “regrap.htm”. Modifications to this file were minor and consisted solely in decreasing the minimum allowable values for the extrusion and speed multiplier sliders of the user interface from 50 to 1 %. These features may be useful in determining optimal gel extrusion rates but are not necessary for the proper working of the paste extruder. The modifications were made on lines 2350 and 2372 of the file. A copy of our modified interface.js file can be supplied on request.

Preparation of LMWG solutions and gels: The two LMWG were synthesized as described previously.^{1,2} Low molecular weight gelator solutions were prepared in different ways depending on their gelation trigger. The gelator solutions for the pH switch gels were prepared by weighing out 25 mg of gelator (5 mg mL^{-1}) into 14 mL vials then, while stirring, adding deionised H_2O and $\text{NaOH}_{(\text{aq})}$ (1 eq.) to a total volume of 5 mL and stirring overnight. Then, glucono- δ -lactone (GdL) was preweighed into 10 mL polypropylene syringes (8 mg/mL). The gelator solutions were transferred in through the nozzle of the syringes via a needle and the syringes were left standing upright to gel overnight. The pH-triggered gels reached a final pH of 3.6. The gelator solutions for the solvent switch gels were prepared by weighing out 25 mg of gelator (5 mg/mL) into 14 mL vials then adding 1.5 mL dimethyl sulfoxide (DMSO). The DMSO gelator solution was sonicated in an ultrasonic bath for a few minutes until the gelator was dissolved. The DMSO solution was then transferred to a 10 mL polypropylene syringe and 3.5 mL H_2O at pH 6 was then added to the DMSO solution and left to gel overnight. The solvent-triggered gels had a final pH of 6.0.

pH measurements: A FC200 pH probe from HANNA instruments with a 6 mm \times 10 mm conical tip was used for pH measurements. pH measurements were carried out on the solutions prior to gelation and on the gels post-measurement.

Rheological measurements: Rheological measurements were performed on an Anton Paar Physica MCR301 rheometer utilising a 25 mm sandblasted parallel plate geometry. Sand paper was attached to the bottom plate to prevent wall slippage for the recovery tests where a higher shear rate was applied. 3 mm thick slices of gels were carefully removed from the syringe they had formed in and then transferred to the rheometer. For the rheological measurements of extruded gels, gels were

manually extruded directly onto the rheometer plate into a circular mould. In all cases the rheometer plate was lowered to the top of the gel which was a gap of approximately 3 mm.

For shear sweep measurements, a constant frequency of 10 rad/s was applied and the shear rate (s^{-1}) was ramped from 0 to 100. For frequency sweeps a shear rate of $0.02 s^{-1}$ was used which was within the linear viscoelastic region of the strain sweeps and the angular frequency was ramped from 1 to 100 rad/s. For compressions tests a constant shear rate of $0.02 s^{-1}$ as applied while the gap distance decreased at a constant rate of $10 \mu m/s$.

Confocal Microscopy: Confocal Microscopy images were taken using a Zeiss LSM 710 confocal microscope with a LD EC Epiplan NEUFLUAR 50x (0,55 DIC) objective. Samples were stained with Nile Blue and excited at 634 nm using a He-Ne laser with the emission detected between 650 and 710 nm. Gels were prepared in disposable Greiner Bio-One CELLviewTM 35 mm plastic cell culture dishes with a glass bottom. Extruded gels were prepared in a syringe then extruded into the cell culture dish shortly before imaging. To stain the pH switch gels with Nile Blue, a 0.1 wt% Nile Blue solution was prepared and added to the gelator solution at $2 \mu L/mL$. To stain the solvent switch gels the Nile Blue was mixed with the water and added to the DMSO gelator solution to a final Nile Blue concentration of $2 \mu L/mL$.

Small Angle Neutron Scattering (SANS): SANS measurements of the gelator solutions were performed using the SANS2D time-of-flight diffractometer (STFC ISIS Pulsed Neutron Source, Oxfordshire, UK).³ A simultaneous Q-range [$Q = 4\pi \sin(\theta/2)/\lambda$, where θ is the scattering angle] of 0.005 to 0.7 \AA^{-1} was achieved using an incident wavelength (λ) range of 1.75 to 16.5 \AA and employing a sample-to-detector distance of 4 m, with the 1 m^2 detector offset vertically 60 mm and sideways 100 mm. The incident neutron beam was collimated to 8 mm diameter. Samples were housed in 2 mm pathlength quartz cuvettes and measured for 60 minutes each. The 'raw' scattering data were normalised to the incident neutron wavelength distribution, corrected for the linearity and efficiency of the detector response and the measured neutron transmission (*i.e.*, absorbance) using the Mantid framework.^{4,5} They were then placed on an absolute scale by comparison with the expected scattering from a partially-deuterated polystyrene blend of known composition and molecular weights in accordance with established procedures.⁶ The background scattering from a quartz cell containing D_2O or 30 vol% d_6 -DMSO in D_2O was then subtracted. The resulting 'reduced' scattering data were then fitted to a customised model comprising of a (Kratky-Porod) flexible cylinder and an absolute power law in the SasView software (version 4.1.1).⁷⁻⁹ The power law (Q^{-m}) accounts for the mass fractal contribution to the scattering intensity which is combined with the flexible cylinder and sphere models.

Ultra Small Angle Neutron Scattering (USANS): USANS measurements of the gelator solutions were performed using the BT5 instrument (NIST Center for Neutron

Research (NCNR), National Institute for Standards and Technology (NIST), Gaithersburg, MD, USA). A Q-range [$Q = 4\pi \sin(\theta/2)/\lambda$, where θ is the scattering angle] of 0.00003 to 0.0011 \AA^{-1} was achieved using a Bonse-Hart type double crystal diffractometer with a wavelength (λ) of 2.4 \AA ($\Delta\lambda/\lambda=6\%$) in the standard geometry.¹⁰ Samples were housed in 5 mm quartz cuvettes and measured for 4h each. Scattering data were normalized for the sample transmission and background corrected using a quartz cell containing D₂O or 30 vol% d₆-DMSO in D₂O.¹¹

The data was reduced using IGOR Pro.¹¹ The reduced data were then fitted in the SasView software (version 4.1.1)¹² to a customised model comprising of a (Kratky-Porod) flexible cylinder and an absolute power law.⁷⁻⁹ The power law (Q^{-m}) accounts for the mass fractal contribution to the scattering intensity which is combined with the flexible cylinder model. As there was no overlap between the USANS and SANS data, the USANS data and fits were manually offset in the y-axis by +20 for **1a**, +500 for **1b**, +150 for **2a** and +250 for **2b** for visual representation. Data were fitted before any post-modification was applied.

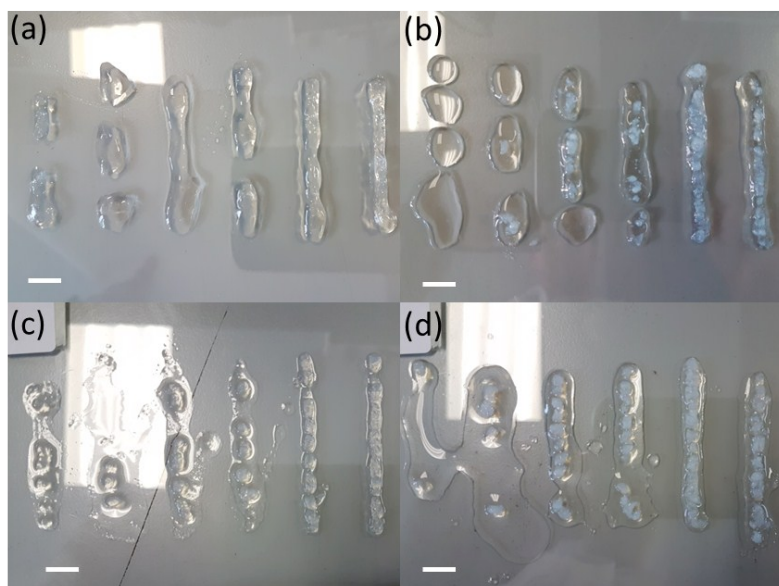


Figure S8. Automatically extruded lines of gels (a) **1a**; (b) **1b**; (c) **2a**; (d) **2b** at set shear rates. pH-triggered gels **1b** and **2b** gels were extruded with double the shear rate. Lines are (left to right) 1094, 1094, 3322, 3322, 16612 and 16612 s^{-1} for (a) and (c) and 2208, 2208, 6645, 6645, 33224 and 33224 s^{-1} for (b) and (d). Lines in (a) and (c) contain 200 μL gel and lines in (b) and (d) contain 400 μL gel. Scale bar 1 cm in all cases.

Gel	Volume / $\mu\text{L}/\text{cm}$	Speed / mm/min	Time taken to print 5 cm line / s	Shear Rate / s^{-1}
1a	40	15,000	0.24	19,894
1b	80	15,000	0.24	39,789
2a	40	15,000	0.24	19,894
2b	80	15,000	0.24	39,789

Table S1. Optimal parameters for printing gels 1a, 1b, 2a and 2b.

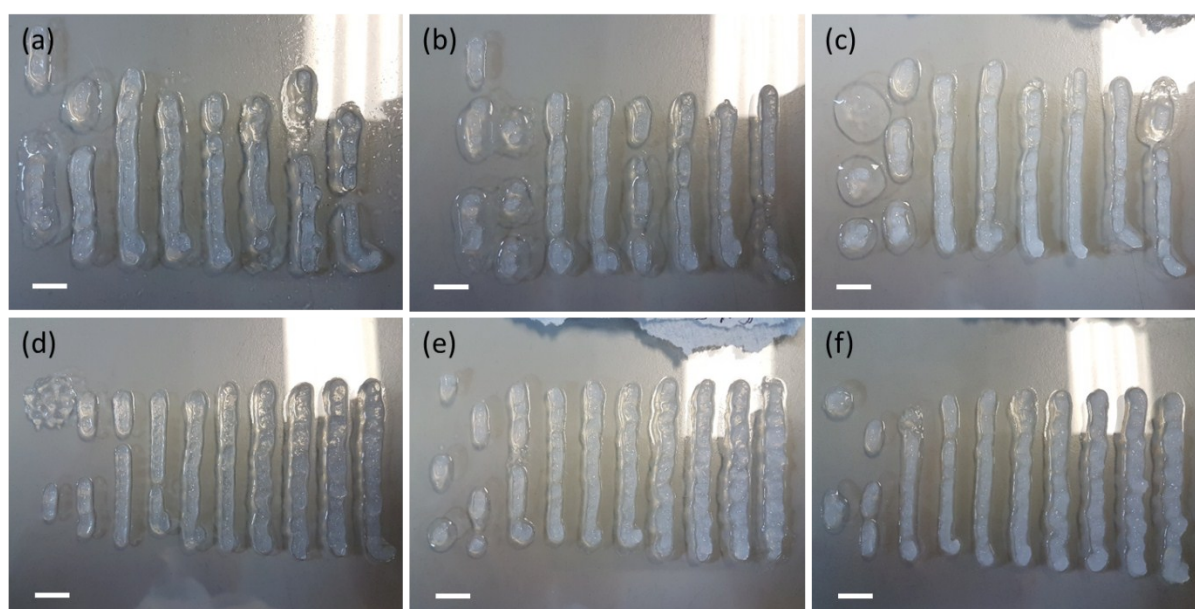


Figure S9. Photographs of lines of **2a** at (a, d) 5, (b, e) 7.5 and (c, f) 10 mg/mL concentrations printed using different parameters to find the optimal line. (a-c) Constant volume of 40 $\mu\text{L}/\text{cm}$ and, from left to right, speeds of 10k, 10k, 15k, 15k, 20k, 20k, 25k and 25k mm/min . (d-f) Constant speed of 15 mm/min and, from left to

right, volumes of 10, 20, 30, 40, 50, 60, 70, 80, 90 and 100 $\mu\text{L}/\text{cm}$. Scale bars are 1cm in all cases.

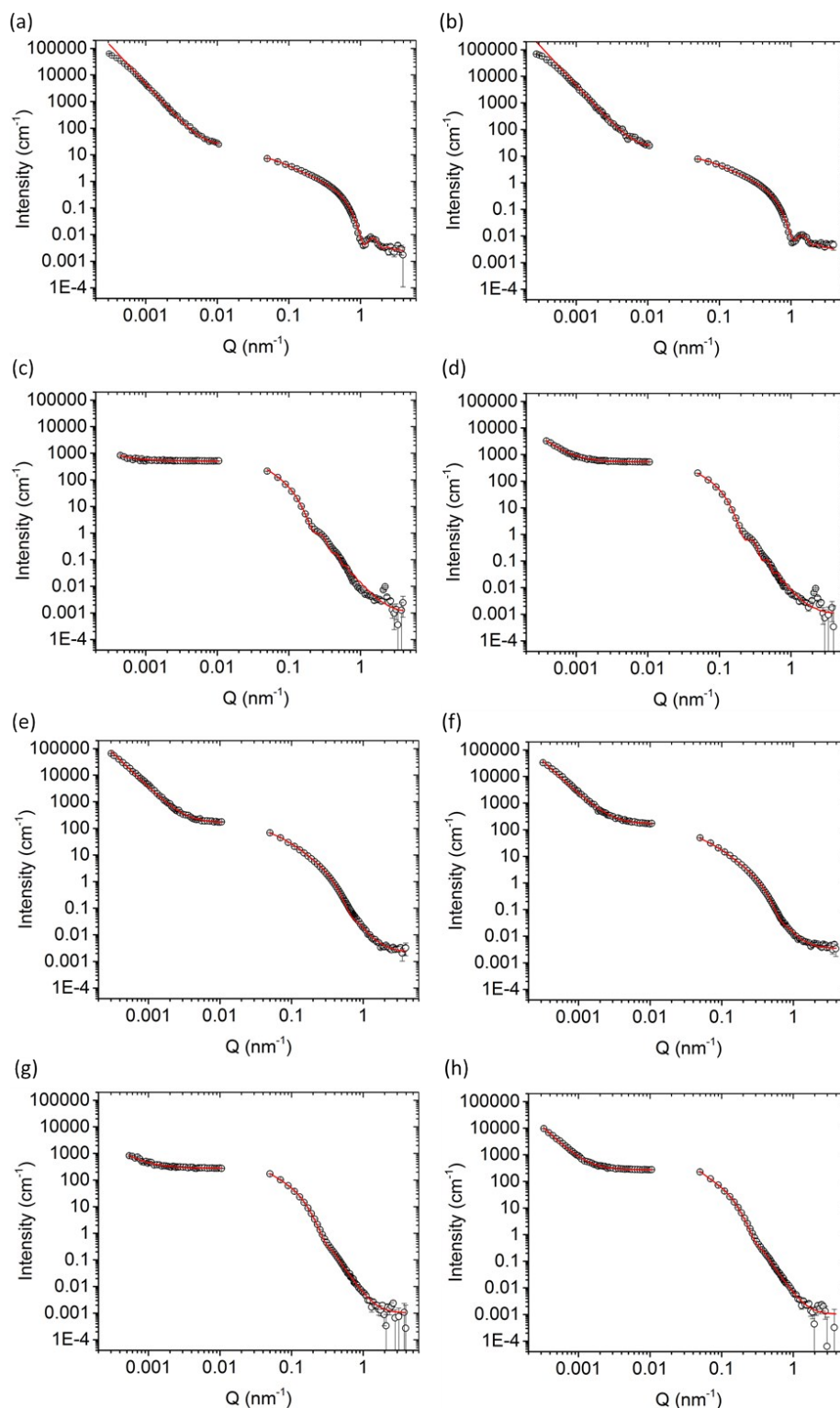


Figure S10. SANS and USANS data of (a) **1a**; (b) **1a** after extrusion; (c) **1b**; (d) **1b** after extrusion; (e) **2a**; (f) **2a** after extrusion; (g) **2b**; (h) **2b** after extrusion. The scatter with error indicates the scattering data and the red lines are the modelled fits of the data where SANS and USANS were fitted separately.

(a)

	USANS							
	1a	1a Extruded	1b	1b Extruded	2a	2a Extruded	2b	2b Extruded
p1_background (cm ⁻¹)			0.002	0.002	0.002	0.002	0.002	0.002
p1_kuhn_length (nm)			10	10	10	10	10	10
p1_length (nm)			100	100	100	100	100	100
p1_radius (nm)			2	2	2	2	2	2
p1_scale (x10 ⁻³)	0	0	0.04	0.091	0.04	0.04	0.078	0.075
p1_sld (x10 ⁶ Å ⁻²)			2.17	2.17	2.17	2.17	2.17	2.17
p1_sld_solvent (x10 ⁶ Å ⁻²)			6.27	6.27	6.27	6.27	6.27	6.27
p2_power	3.9	3.9	2.72	3.1	3.57	3.44	2.8	3.5
p2_scale (x10 ⁻⁴)	1.70E-09	1.70E-09	0.000001	0.0000018	0.00000025	0.00000051	0.00000125	0.00000008
scale_factor			1	1	1	1	1	1
Radius PD			0	0	0	0	0	0

(b)

	SANS							
	1a	1a Extruded	1b	1b Extruded	2a	2a Extruded	2b	2b Extruded
p1_background (cm ⁻¹)	0.002	0.002	0.00101	0.00101	0.0021	0.0034	0.00101	0.00101
p1_kuhn_length (nm)	50	50	36	36	12	12	26	26
p1_length (nm)	90	70	100	100	230	230	100	100
p1_radius (nm)	3.4	3.5	18	18	5.5	5.5	13	13
p1_scale (x10 ⁻³)	1.85	2.15	1.45	1.45	2.40	1.50	1.80	2.00
p1_sld (x10 ⁶ Å ⁻²)	2.17	2.17	2.17	2.17	2.17	2.17	2.17	2.17
p1_sld_solvent (x10 ⁶ Å ⁻²)	6.27	6.27	6.27	6.27	6.27	6.27	6.27	6.27
p2_power	1	1	2.9	2.9	2.3	2.5	3.3	3.4
p2_scale (x10 ⁻⁴)	2	5	0.14	0.07	0.3	0.13	0.01	0.01
scale_factor	1	1	1	1	1	1	1	1
Radius PD	0	0	0	0	0.2	0.2	0.2	0.2

Table S2. Derived fit parameters for (a) USANS and (b) SANS data fitted to the Kratky-Porod flexible cylinder (contribution p1) plus power law (contribution p2) model. For details of the meaning of the parameters the reader is referred to the SasView model documentation at www.sasview.org. The data shown in bold is to clarify where changes were made in the fits between the original and extruded counterparts of each gel.

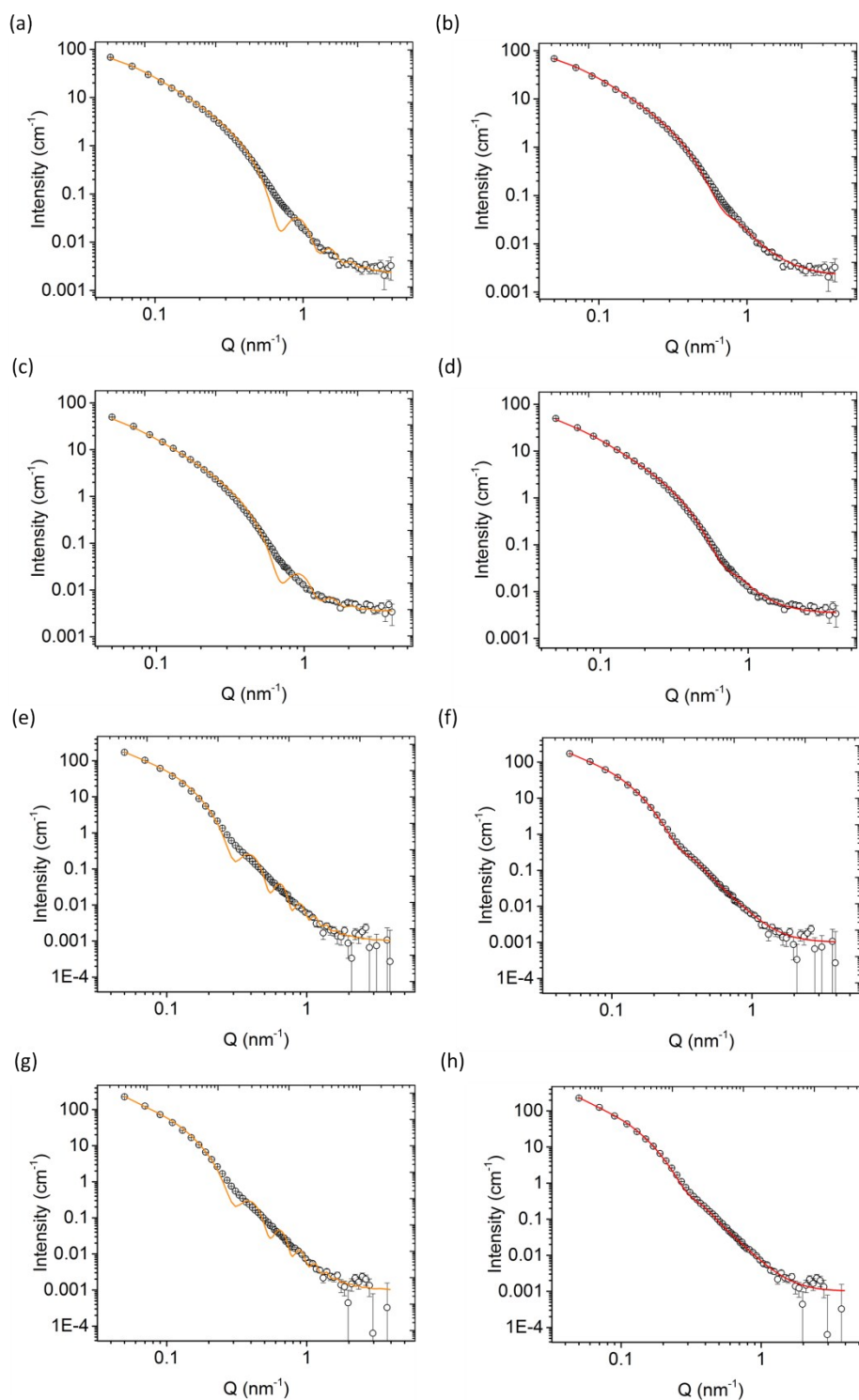


Figure S11. SANS data and fits showing the use of radius polydispersity (pd) in the fits of **2a** and **2b**, before and after extrusion. Defining features in the scatter were fitted first with no polydispersity, then $pd(\text{radius})=0.2$ was added to broaden the features from the model. (a) **2a** $pd(\text{radius})=0$; (b) **2a** $pd(\text{radius})=0.2$; (c) **2a** after extrusion $pd(\text{radius})=0$; (d) **2a** after extrusion $pd(\text{radius})=0.2$; (e) **2b** $pd(\text{radius})=0$; (f) **2b** $pd(\text{radius})=0.2$; (g) **2b** after extrusion $pd(\text{radius})=0$; (h) **2b** after extrusion $pd(\text{radius})=0.2$. Scatters are data with y errors and lines are model fits.

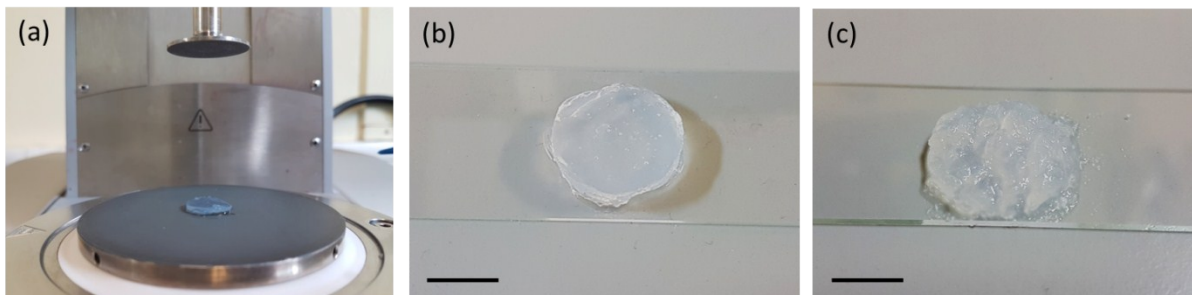


Figure S12. (a) Photograph of a slice of the gel on the rheometer plate with the pp25/s measuring system ready to be lowered. For recovery strain tests, the bottom plate was covered with sandpaper to prevent wall slipping. (b) Original gel and (c) extruded gel examples on glass slides before rheology tests. Scale bar 1cm in all cases.

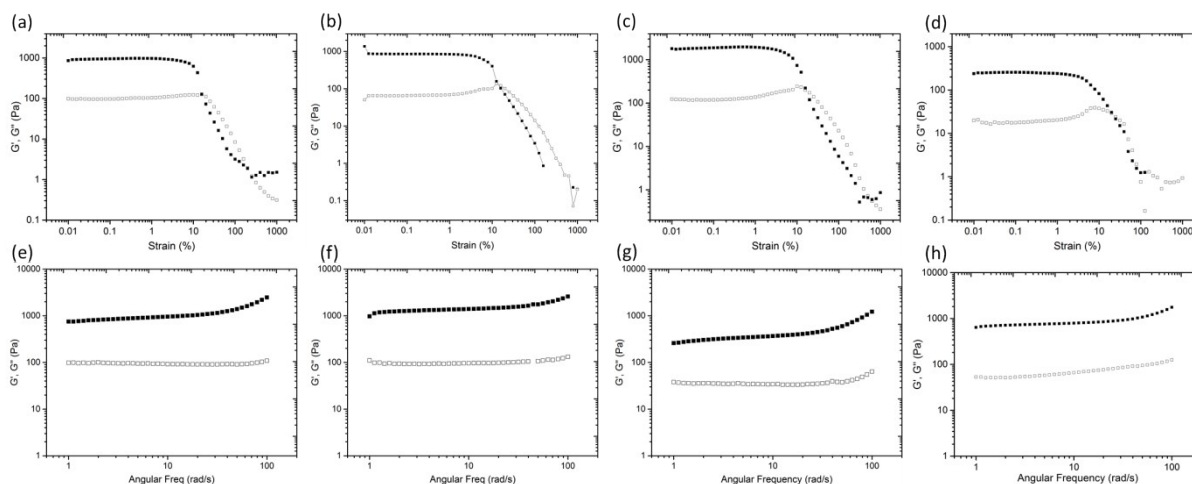


Figure S13. Strain (a-d) and frequency (e-h) sweeps of gels before extrusion (a, e) **1a**; (b, f) **1b**; (c, g) **2a**; (d, h) **2b**. Frequency sweeps were run at a strain of 0.2 %. Open circles represent G'' and solid circles represent G' .

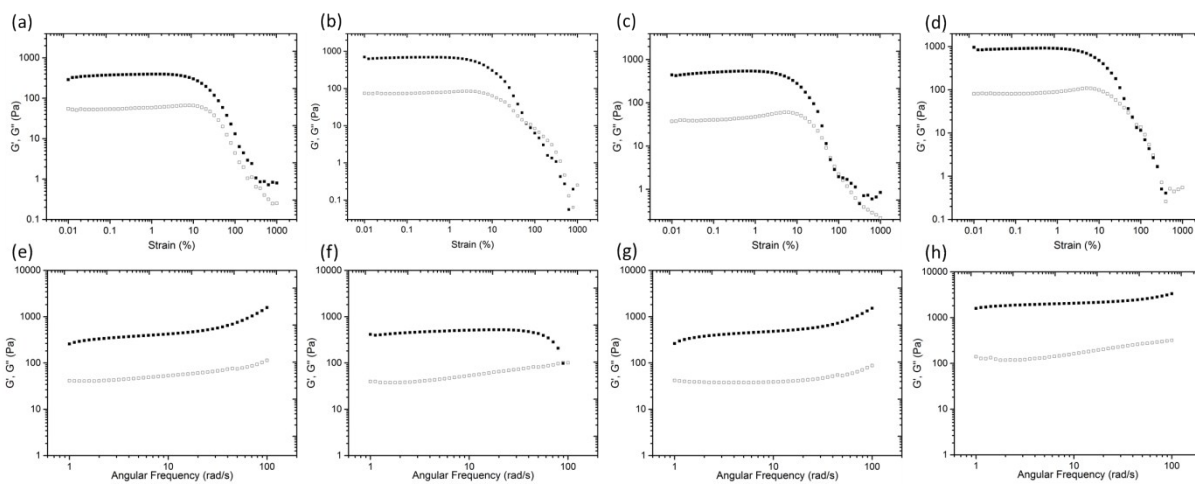


Figure S14. Strain (a-d) and frequency (e-h) sweeps of gels after extrusion (a, e) **1a**; (b, f) **1b**; (c, g) **2a**; (d, h) **2b**. Frequency sweeps were run at a strain of 0.2 %. Open circles represent G'' and solid circles represent G' .

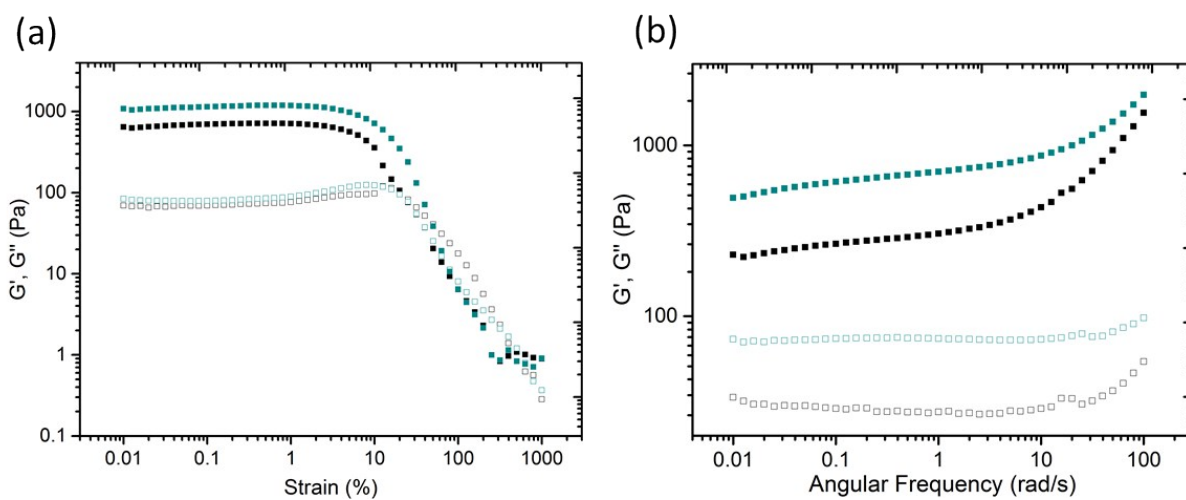


Figure S15. (a) Strain sweeps and (b) frequency sweeps of **2a** before (black) and after compression during printing (blue). Frequency sweeps were run at a constant strain of 0.2 %. Open circles represent G'' and solid circles represent G' .

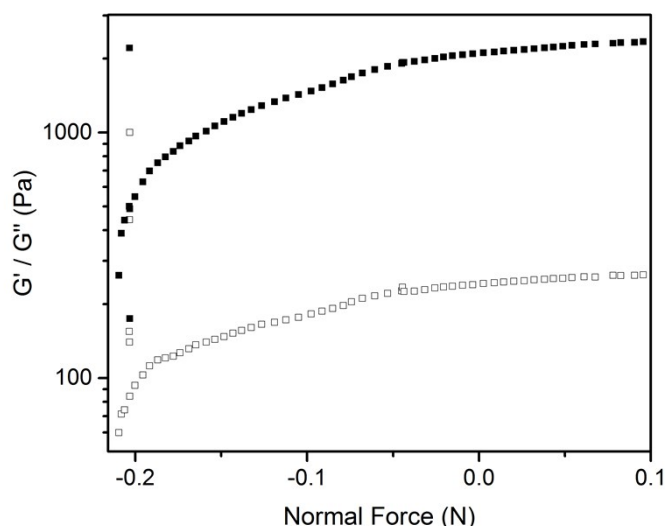


Figure S16. Compression sweep on gel **2a** where the gap between the parallel plate measuring system and base plate was decreased by 10 $\mu\text{m/s}$ while applying a constant strain of 0.2 %. Open circles represent G'' and solid circles

References

- 1 J. Gupta, D. J. Adams and N. G. Berry, *Chem. Sci.*, 2013, **0**, 1–3.
- 2 D. J. Adams, M. F. Butler, W. J. Frith, M. Kirkland, L. Mullen and P. Sanderson, *Soft Matter*, 2009, **5**, 1856.
- 3 <http://isis.stfc.ac.uk/>, .
- 4 O. Arnold, J. C. Bilheux, J. M. Borreguero, A. Buts, S. I. Campbell, L. Chapon, M. Doucet, N. Draper, R. Ferraz Leal, M. A. Gigg, V. E. Lynch, A. Markvardsen, D. J. Mikkelson, R. L. Mikkelson, R. Miller, K. Palmen, P. Parker, G. Passos, T. G. Perring, P. F. Peterson, S. Ren, M. A. Reuter, A. T. Savici, J. W. Taylor, R. J. Taylor, R. Tolchenov, W. Zhou and J. Zikovsky, *Nucl. Instruments Methods Phys. Res. Sect. A Accel. Spectrometers, Detect. Assoc. Equip.*, 2014, **764**, 156–166.
- 5 <http://www.mantidproject.org/>, .
- 6 G. D. Wignall and F. S. Bates, *J. Appl. Crystallogr.*, 1987, **20**, 28–40.
- 7 A Guinier and G. Fournet, *John Wiley Sons, Inc., New York*, 1955, 18, 1–19.
- 8 J. S. Pedersen and P. Schurtenberger, *Macromolecules*, 1996, **29**, 7602–7612.
- 9 W. R. Chen, P. D. Butler and L. J. Magid, *Langmuir*, 2006, **22**, 6539–6548.
- 10 A. R. Drews, J. A. Barker, C. J. Glinka and M. Agamalian, *Phys. B*, 1998, **241–243**, 241–243.

- 11 S. R. Kline, *J. Appl. Crystallogr.*, 2006, **39**, 895–900.
- 12 www.sasview.org.